analytical chemistry

pubs.acs.org/ac Article

Feasibility of Applying Fourier Transform Electrochemical Impedance Spectroscopy in Fast Cyclic Square Wave Voltammetry for the *In Vivo* Measurement of Neurotransmitters

Cheonho Park, Sangmun Hwang, Yumin Kang, Jeongeun Sim, Hyun U. Cho, Yoonbae Oh, Hojin Shin, Do Hyoung Kim, Charles D. Blaha, Kevin E. Bennet, Kendall H. Lee, and Dong Pyo Jang*

Cite This: *Anal. Chem.* 2021, 93, 15861−15869 Read Online

ACCESS | Metrics & More | Article Recommendations | Supporting Information

ABSTRACT: We previously reported on the use of fast cyclic square wave voltammetry (FCSWV) as a new voltammetric technique. Fourier transform electrochemical impedance spectroscopy (FTEIS) has recently been utilized to provide information that enables a detailed analytical description of an electrified interface. In this study, we report on attempts to combine FTEIS with FCSWV (FTEIS−FCSWV) and demonstrate the feasibility of FTEIS−FCSWV in the *in vivo* detection of neurotransmitters, thus giving a new type of electrochemical impedance information such as biofouling on the electrode surface. From FTEIS−FCSWV, three new equivalent circuit element voltammograms, consisting of charge-transfer resistance (R_{ct}), solution-resistance (R_s), and double-layer capacitance (C_{dl}) voltammograms were constructed and investigated in the phasic changes in dopamine (DA) concentrations. As a result, all R_{ct}, R_s, and C_{dl} voltammograms showed different DA redox patterns and linear trends for the DA concentration ($R^2 > 0.99$). Furthermore, the R_{ct} voltammogram in FTEIS−FCSWV showed lower limit of detection (21.6 ± 15.8 nM) than FSCV (35.8 ± 17.4 nM). FTEIS−FCSWV also showed significantly lower prediction errors than FSCV in selectivity evaluations of unknown mixtures of catecholamines. Finally, C_{dl} from FTEIS−FCSWV showed a significant relationship with fouling effect on the electrode surface by showing decreased DA sensitivity in both flow injection analysis experiment ($r = 0.986$) and *in vivo* experiments. Overall, this study demonstrates the feasibility of FTEIS−FCSWV, which could offer a new type of neurochemical spectroscopic information concerning electrochemical monitoring of neurotransmitters in the brain, and the ability to estimate the degree of sensitivity loss caused by biofouling on the electrode surface.

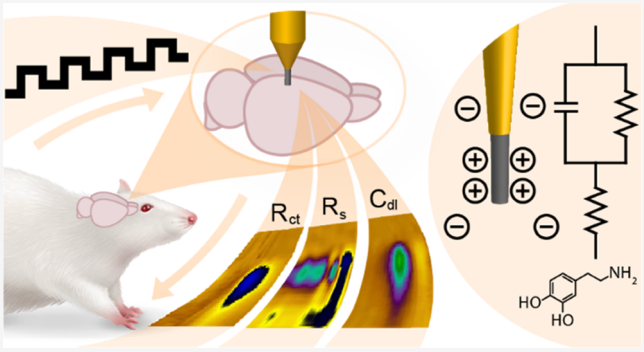

INTRODUCTION

Electrochemical impedance spectroscopy (EIS) allows a comprehensive description of an electrode and an electrolyte interface with an equivalent circuit for a given electron-transfer reaction. It provides information that is needed to describe the electrified interface, including Faradic and non-Faradic processes, along with the electrolyte solution by estimating the equivalent circuit model.[1−3] Thus, EIS has been applied to studies dealing with corrosion reactions,[4,5] the characterization of electrodes,[6] and biosensors.[7] EIS measurements typically involve the use of a frequency response analyzer, which generates a series of AC waves with various frequencies, applies the waveform to the electrochemical system of interest, and measures the current responses at each designated frequency. The measured current responses are then analyzed to obtain an impedance spectrum and equivalent circuit elements, such as charge-transfer resistance or capacitance. However, this approach involves scanning the whole range of frequencies, making it a time-consuming process. In the inclusion of low-frequency information below 1.0 Hz, EIS requires at least a few minutes of scanning time for each frequency. This feature has led a number of researchers to develop more rapid methods for EIS measurements. For example, Smith et al. used a multisine signal obtained by mixing several AC voltages of various frequencies.[8] The resulting current was converted into AC currents of the corresponding frequencies. The impedances were then obtained for the frequencies that were used to assemble the composite signal after the current signal was deconvoluted by Fourier transform. This advanced approach is referred to as Fourier transform electrochemical impedance spectroscopy (FTEIS).[9]

Received: June 1, 2021
Accepted: November 16, 2021
Published: November 29, 2021

https://doi.org/10.1021/acs.analchem.1c02308
Anal. Chem. 2021, 93, 15861−15869

FTEIS based on multisine excitation measurements has been improved upon so as to provide much faster impedance measurements that utilize small potential steps and is referred to as second-generation FTEIS.[10] It was applied to an electrochemical system as an integrated form of the Dirac δ function, followed by converting derivative signals of the stepped potential and the resulting current into AC voltages and currents in a full frequency range, leading to a full range of an impedance spectrum by Fourier transform. Researchers have attempted to develop time-resolved EIS for further development as the speed of recording EIS spectra increases.[11−13] One of such techniques is staircase cyclic voltammetric FTEIS (SCV-FTEIS), a relatively faster measurement method during a potential sweep by combining FTEIS with the staircase cyclic voltammetric experiment.[11] A staircase cyclic voltammogram (SCV) is obtained by collecting sampled currents at various DC voltage levels during their chronoamperometric current decay after applying a series of small ascending or descending small potential steps. The step signal is an integrated form of the Dirac δ function, which is obtained by summing the AC voltages of all frequencies. In SCV-FTEIS, derivative signals received from both the recorded voltage and current signals are deconvoluted into AC voltages, and the currents are deconvoluted into the frequency domain by Fourier transform. Since the SCV experiment records a series of chronoamperometric currents, all of the information necessary to describe the system can be extracted from a single pass in the SCV experiment by means of FTEIS analyses of the stepped potentials and the resulting currents.[14−16] This offers a number of advantages to investigators who are running electrochemical experiments as they are much more familiar with a linear sweep or cyclic voltammetry.[9,17,18]

Despite the superior advantages of SCV-FTEIS, only a few studies have utilized SCV-FTEIS to detect neurochemical changes in the brain. This may be due to the slow scan rate (a few hundred millivolts per second) employed, which is at least two orders of magnitude slower than the timeframe of 1−10 s of milliseconds for neurotransmission (release).[9] For detecting extracellular changes in neurochemicals in the brain, where concentration changes are in the subsecond level, a high temporal resolution (<1 s) is required, such as fast-scan cyclic voltammetry (FSCV), which is frequently used in neurochemical measurements *in vivo*. FSCV is used to measure neurochemicals via the use of a relatively high scan rate (>400 V/s), subsecond resolution (100 ms), while also providing excellent chemical selectivity and sensitivity.[19]

In a previous study, we reported the development of fast cyclic square wave voltammetry (FCSWV) to measure neurotransmitters with higher sensitivity and selectivity than FSCV.[20] FCSWV rapidly repeats a square wave voltammetric waveform composed of a staircase waveform with repeated two equal magnitudes and opposite direction square wave pulses. The waveform is repeated at 5 Hz to satisfy the temporal resolution requirement of neurotransmitter measurements *in vivo*. The voltammogram can be reconstructed as a two-dimensional (2D) voltammogram to produce high sensitivity and selectivity. We assumed that an FTEIS analysis could be combined with FCSWV because the applied waveforms are similar. In this study, we report on developing a new electrochemical impedance voltammetric technique (FTEIS−FCSWV) by combining FTEIS with FCSWV. Using FTEIS−FCSWV, equivalent circuit element voltammograms that include charge-transfer resistance (R_{ct}), solution-resistance (R_s), and double-layer capacitance (C_{dl}) voltammograms can be reconstructed as new electrochemical features in addition to the FCSWV voltammogram.

In addition, we investigate the feasibility of double-layer capacitance (C_{dl}) as an indicator for biofouling, which is the degree of sensitivity loss caused by the change in the electrode surface *in vivo*. The thickness of the double layer can be affected by the biofilm formation on the electrode surface, resulting in the change in double-layer capacitance (C_{dl}).[21−24] Therefore, in this study, the relationship between biofouling degree and double-layer capacitance is presented using FTEIS−FCSWV.

EXPERIMENTAL SECTION

Data Acquisition. Data were acquired with a commercial electronic interface (NI USB-6356, 16-bit, National Instruments) with a base-station PC and the software written in the LabVIEW programming environment (National Instruments, Austin, TX). A current-to-voltage converting preamplifier without any analog filter was used to preserve frequency information in the square wave pulse in FCSWV. After data collection, all waveform parameters and operations, data acquisition and transmission, background subtraction, and signal averaging were performed with custom software control. Data were saved to the hard drive of a base-station computer for offline processing in MATLAB (MathWork Inc., Natick, MA). Parallel computing, which uses multiple processors to compute the task, was adopted to increase computational efficiency. A detailed introduction to the parallel computing concept is shown in Figure S-1. GraphPad Prism (GraphPad Software, San Diego, CA) was used to generate figures and statistics. All data, except for voltammograms, are presented as the mean ± standard deviation (SD) for "*n*" electrodes. The same group of electrodes was used for comparisons between FSCV and FTEIS−FCSWV.

Fast-Scan Cyclic Voltammetry. A conventional FSCV waveform[25] was used to compare with the performance of FTEIS−FCSWV using the same in-house made experimental setup described above. A scan rate of 400 V/s and a holding potential of −0.4 V versus Ag/AgCl were used. The switching potential was 1.3 V, and waveforms were repeated with 3 Hz to match the FTEIS waveforms.

Electrodes. Carbon-fiber microelectrodes (CFM) were fabricated as previously described.[26,27] An AS4 carbon fiber (d = 7 μM, Hexel, Stamford, CT) was used in all experiments. The exposed carbon fiber was trimmed to a final length of 70−120 μm with a scalpel. The Ag/AgCl reference electrode was fabricated by chlorinating 1 mm of the bare end of a 31 gauge silver wire (PFA coated 030″, bare 025″, A-M Systems). Supporting Information includes a detailed description of the electrode fabrication process. (Figure S-2)

Chemicals. DA, norepinephrine (NE), and epinephrine (EP) were dissolved at a stock concentration of 1 mM in Tris buffer (15 mM tris(hydroxymethyl)aminomethane, 3.25 mM KCl, 140 mM NaCl, 1.2 mM $CaCl_2$, 1.25 mM NaH_2PO_4, 1.2 mM $MgCl_2$, and 2.0 mM Na_2SO_4, pH 7.4). The stock solution was diluted to the final concentration in Tris buffer before starting the flow injection experiments. All chemicals, including nomifensine, were purchased from Sigma-Aldrich (St. Louis, MO). The oxidation of the neurotransmitters in the stock solutions was prevented by sparging the stock solutions with nitrogen from a gas vessel.

https://doi.org/10.1021/acs.analchem.1c02308
Anal. Chem. 2021, 93, 15861−15869

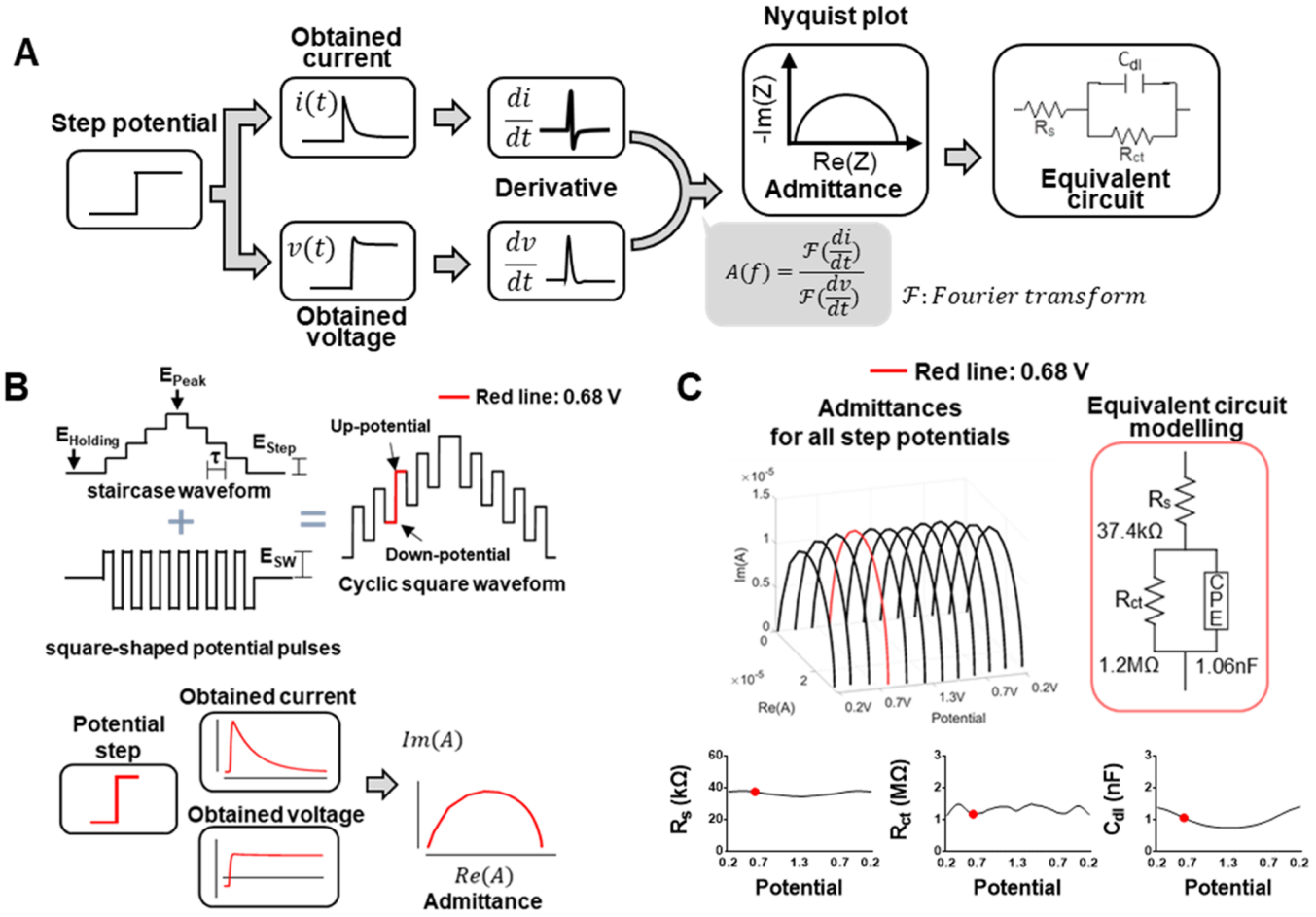

Figure 1. Scheme for FTEIS and FTEIS−FCSWV. (A) Basic concept of FTEIS. FTEIS uses a step potential as a perturbation signal. FTEIS analysis obtains voltage and current information to allow a full impedance spectrum to be produced and the equivalent circuit elements. (B) Application of FTEIS into FCSWV. Each potential step is analyzed as an integrated form of the Dirac δ function in FTEIS. The red line (0.68 V) was added to indicate how a specific potential step was analyzed. (C) Estimation of the element value of the equivalent circuit from the admittance data and the reconstruction of three new types of component voltammograms: charge-transfer resistance (R_{ct}) voltammogram, solution-resistance (R_s) voltammogram, and double-layer capacitance (C_{dl}) voltammogram.

Principal Component Regression Analysis. To compare the selectivity against neurotransmitters between FTEIS−FCSWV and FSCV, principal component regression (PCR) analysis was conducted with MATLAB.[25,28] To prepare the PC regression matrix, 0.5, 1.0, 1.5, and 2.0 μM DA and NE were analyzed. Data for 1.0, 2.0, 3.0, and 4.0 μM were obtained for EP. Each solution was measured with both FSCV and FTEIS−FCSWV. The number of principal components was chosen to explain 99.5% of the original data. To confirm that the regression matrix was constructed precisely, half of the obtained data were used as a training set, and the other half was used as a test set. Voltammograms of unknown mixtures were evaluated to verify the predictive ability of the constructed regression matrix.

***In Vivo* Experiments.** Adult male Sprague-Dawley rats (8−9 weeks old, weighing 250−300 g, Koatech, South Korea) were used for this study (n = 3). The rats were housed in 12 h light/dark cycles and were given food and water *ad libitum*. US National Institutes of Health (NIH) guidelines were followed for animal care, and the Hanyang University Institutional Animal Care and Use Committee approved the experimental procedures. Rats were anesthetized by intraperitoneal injection (anesthetic urethane, 1.5 g/kg, i.p.). Surgeries were performed using a stereotaxic frame (Model 900, David Kopf Instruments, Tujunga, CA). To evoke DA release, the medial forebrain bundle (from bregma, AP: −4.6 mm, ML: 1.4 mm, from dura, DV: −8.0 ∼ −9.0 mm) was electrically stimulated, and a CFM was inserted into the striatum (AP: 1.2 mm, ML: 2.0 mm, DV: −4.5).

RESULTS AND DISCUSSION

FTEIS−FCSWV Acquisition and Analysis. The FTEIS−FCSWV measurement starts from the step function concept, an integrated Dirac δ function in second-generation FTEIS.[11] The Dirac δ function is obtained by summing the AC voltages of all frequencies. Because it is an ideal function with the instantaneously infinite value at a particular time point "t" and a zero value at the other points, the step function was used for the practical implementation of this method. As shown in Figure 1A, a step signal was applied to a CFM. In this study, the voltage waveform and the current responses were simultaneously stored through two analog-digital converter channels. The recorded voltage waveform is different from the applied voltage waveform because the applied voltage goes through the op-amp to the CFM. After the signal acquisition, derivative signals obtained from the recorded voltage and current signals were deconvoluted into AC voltages. The currents were then deconvoluted into the frequency domain by

https://doi.org/10.1021/acs.analchem.1c02308
Anal. Chem. 2021, 93, 15861−15869

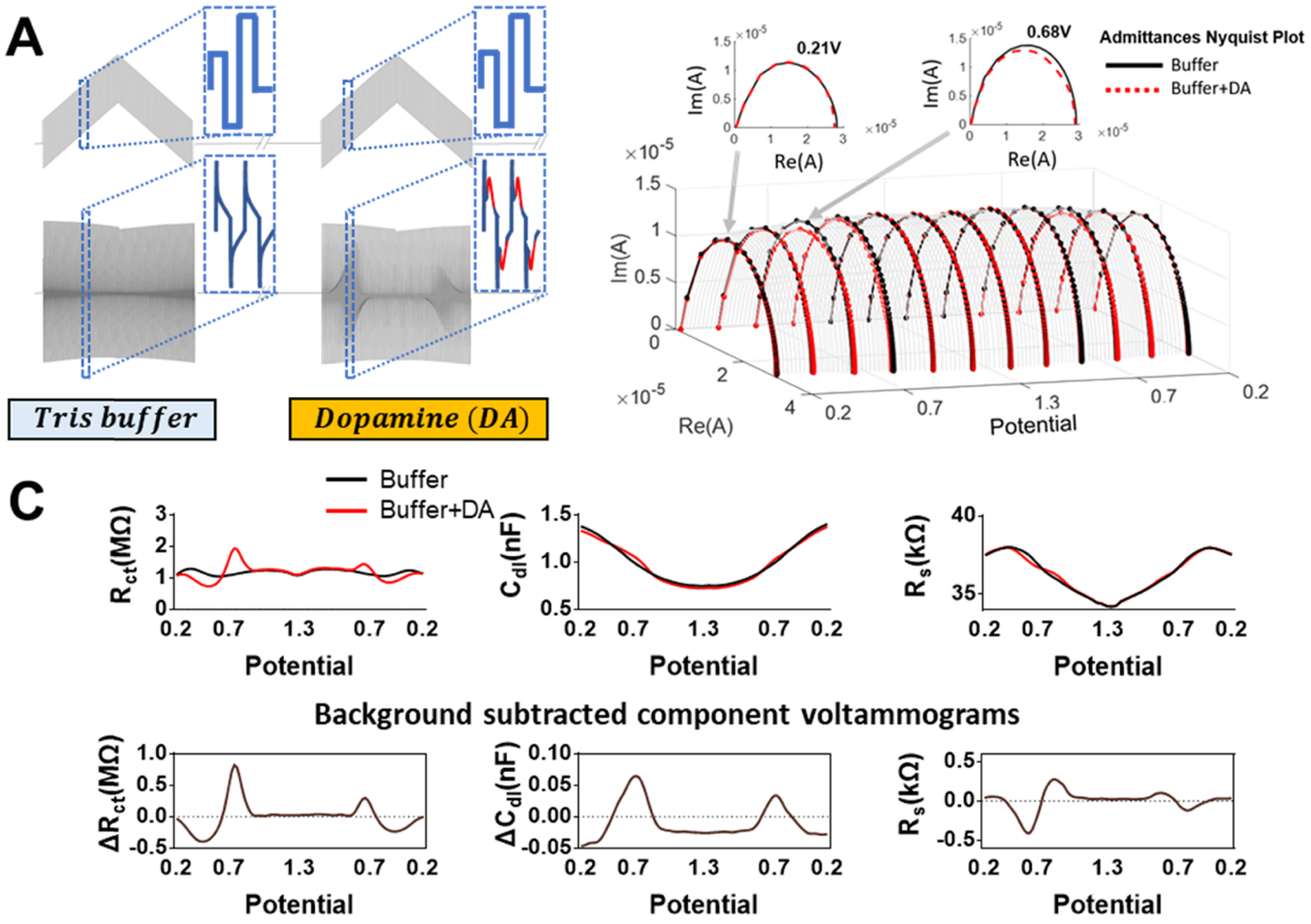

Figure 2. (A) Voltammograms before and after adding dopamine using square wave voltammetry. The blue line components are the conceptual voltage and current and the red line component is the oxidation current of dopamine. (B) Nyquist plots obtained before and after adding 5 μM dopamine to the Tris buffer from the voltammogram (upward direction). Nyquist plots from 0.2/0.7 V magnitude square wave pulses are shown to visualize the change in admittance caused by dopamine. (C) Equivalent circuit element voltammogram of each component in the case of a Tris buffer solution (black line)/dopamine added to the Tris buffer (red line). Background-subtracted element voltammograms of dopamine for each equivalent circuit component are shown below.

Fourier transform. Generally, the impedance at the desired frequency was first obtained by dividing the AC voltage by the current at the frequency in EIS. A full impedance spectrum was then constructed by repeating the calculation through the entire frequency range. This impedance data for all frequency ranges can be visualized with a Nyquist plot and used for the equivalent circuit estimation (Figure 1A).[11] In this study, the equivalent circuit element values were estimated with the admittance (the reciprocal of impedance) instead of impedance, as this empirically provided a more reliable estimate of the performance of the circuit (Figures S-3 and S-4).

For applying the FTEIS into FCSWV, the FCSWV data were acquired with the waveform shown in Figure 1B. As described in our previous study,[20] it consists of a square wave oscillation overlaid on the symmetric staircase waveform. Two equal magnitude and oppositely directed square-shaped potential pulses (upward and downward potentials) are superposed on a single staircase. The staircase potential ramp starts with a holding potential ($E_{Holding}$), increases with each stair step (E_{Step}) up to a peak potential (E_{Peak}), and then decreases back to $E_{Holding}$ (Figure 1B). The waveform parameters used in this study were $E_{Holding}$: −0.2 V, E_{Peak}: 0.9 V, E_{Step}: 0.0224 V, the duration of a single stair step τ: 1 ms, and the magnitude of the upward and downward potentials E_{sw}: 0.4 V. The cyclic square waveform length is 200 ms with 200 stair steps. A sampling rate of 1 MHz was used to collect a sufficient number of data points to permit a Fourier transform analysis in each individual step. The step from downward to upward potential in a staircase ramp was considered a step pulse, an integrated form of the Dirac δ function in FTEIS.[14] In FCSWV, therefore, the admittance could be obtained from each step pulse in FCSWV and a total of 200 admittances from 200 stair steps were visualized with a three-dimensional Nyquist plot for all staircase step potentials (Figure 1C).

To estimate the element value of the equivalent circuit from the admittance data, the MATLAB "Z-fit" fitting function was utilized, which calculates the value of each element of the equivalent circuit through an optimization process.[29] In this study, the modified Randles circuit, which is composed of charge-transfer resistance (R_{ct}), solution-resistance (R_s), and double-layer capacitance (C_{dl}) was used as an equivalent circuit model, as shown in Figure 1C. Charge-transfer resistance, also known as polarization resistance, is the resistance component that arises from an electron transferring reaction. Double-layer capacitance describes the double-layer capacitance of the

https://doi.org/10.1021/acs.analchem.1c02308
Anal. Chem. 2021, 93, 15861−15869

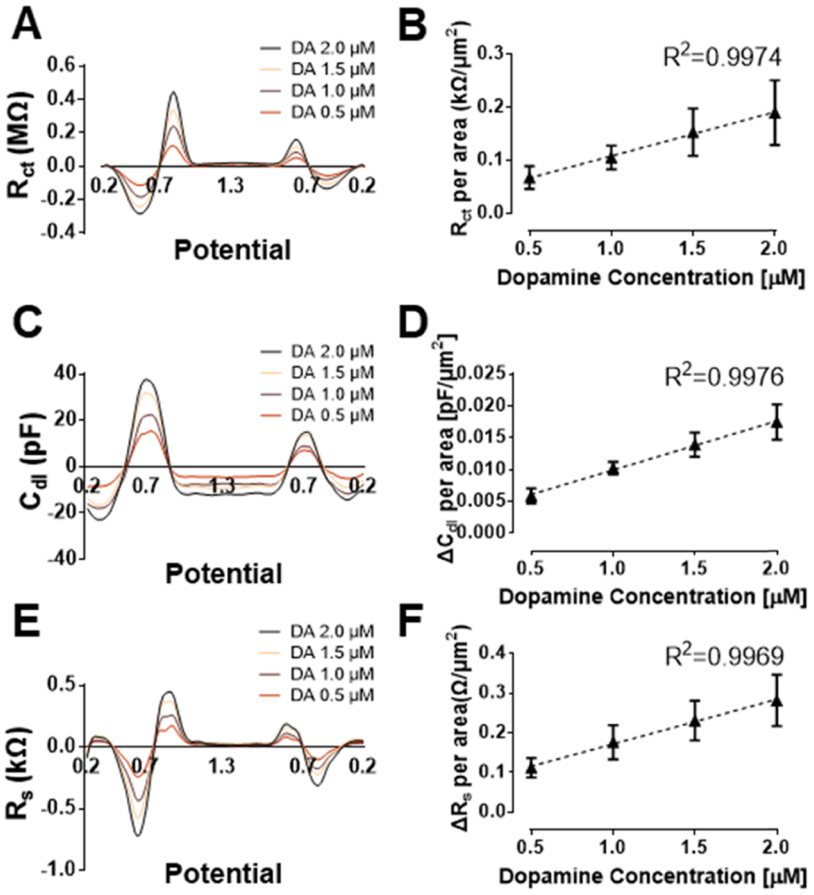

Figure 3. Voltammograms and calibration curve data of each circuit element data. (A) Voltammograms of R_{ct} and (B) its calibration curve. (C) Voltammograms of C_{dl} and (D) its calibration curve. (E) Voltammograms of R_s and (F) its calibration curve. Voltammograms for 0.5, 1.0, 1.5, and 2.0 μM dopamine are shown (n = 5 electrodes used). The element values were divided by each area of electrodes to normalize the difference caused by the difference in the lengths of each carbon-fiber electrode tip.

polarization region near the electrode surface. Solution resistance is the resistance between the electrodes in the ionic solution.[9,30] C_{dl} was obtained from the constant phase element (CPE)[1] described in eq 1[31]

$$C_{dl} = Q_0^{1/n}\left(\frac{R_s * R_{ct}}{R_s + R_{ct}}\right)^{(1-n)/n} \quad (1)$$

where n is the exponent component that describes a phase of CPE and Q_0 is a pseudocapacitance parameter of CPE. A fitting function was applied to find the optimal element values of the Randles circuit model with admittance data at all 200 staircase step potentials (Figure 1C). After obtaining the component values of an equivalent circuit at all staircase step potentials, three new types of component voltammograms could be reconstructed with those estimated component values versus staircase step potentials: a charge-transfer resistance (R_{ct}) voltammogram, solution-resistance (R_s) a voltammogram, and a double-layer capacitance (C_{dl}) voltammogram, as shown in Figure 1C.

Background-Subtracted FTEIS−FCSWV Voltammograms. For EIS measurements, strict criteria such as linearity are required, assuming that there is linearity between the input (voltage, V) and the output (current, I).[32] It is recommended that EIS studies use a small amplitude perturbation (≤10 mV) to guarantee a linear response from the Butler−Volmer model[33] and to be presumed as a pseudolinear relationship instead of nonlinearity.[10,34] In our FTEIS−FCSWV study, the large 800 mV amplitude voltage step was used to cover the oxidation potential and the reduction potential within two equal upward and downward potentials E_{sw}.[20] However, the large amplitude perturbation of FCSWV could not meet the Kramers−Krognig relationship for linearity. Nevertheless, we assumed that equivalent circuit element voltammograms could contain electrochemical information when the electrolytes around an electrode change, such as releasing a neurotransmitter in the brain.

Thus, as a conventional FSCV, we applied a background subtraction method to detect changes in the equivalent circuit element voltammogram during the scanning time by subtracting the reference voltammogram, which was obtained before changing the analyte such as DA.[35] Our thinking was that this background-subtracted equivalent circuit voltammogram could be used as a feature voltammogram in estimating the concentration of the analyte despite the nonlinearity of current−voltage relation in FTEIS−FCSWV. An FTEIS−was investigated with equivalent circuit element voltammograms for use in the detection of DA. As shown in Figure 2A, the FCSWV waveform was repeatedly scanned at a 3.0 Hz frequency for a subsecond measurement, and the current responses to the waveforms were continuously sampled. The change in FCSWV current near the DA oxidation and reduction potential was observed when DA was added to the buffer solution (Figure 2A). The admittances for all staircase

https://doi.org/10.1021/acs.analchem.1c02308
Anal. Chem. 2021, 93, 15861−15869

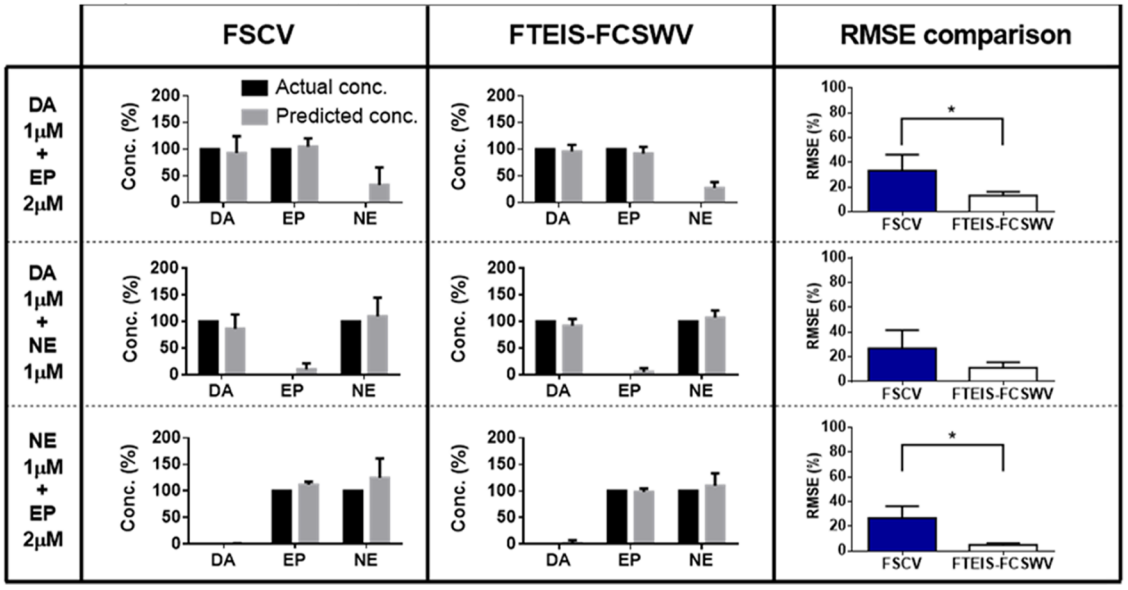

Figure 4. Predictive performance for catecholamines. The neurotransmitter content of solutions containing a mixture was estimated using R_{ct} as a key parameter using principal component regression. The mixture contents are displayed in the left-hand column, and the technique used is displayed in the top row. The predicted concentration is displayed in gray color, and the actual concentration is displayed in black color and set as 100% to visualization. Abbreviations: Conc., concentration; DA, dopamine; EP, epinephrine; NE, norepinephrine; RMSE, root-mean-square error; FSCV, fast-scan cyclic voltammetry; and FTEIS−FCSWV, Fourier transform electrochemical impedance spectroscopy−fast cyclic square wave voltammetry.

step potentials after each FCSWV scan were reconstructed and visualized employing a three-dimensional Nyquist plot, as described in the previous section. When the Nyquist plots were compared before and after the injection of DA, the admittance Nyquist plot was changed at a DA oxidation potential of around the 0.7 V step potential (Figure 2B). By estimating the equivalent circuit following a procedure similar to those for the admittance data, the equivalent circuit element voltammograms were obtained, including the charge-transfer resistance (R_{ct}) voltammogram, solution-resistance (R_s) voltammogram, and a double-layer capacitance (C_{dl}) voltammogram for each FCSWV scan (Figure 2C). To observe the DA responses in equivalent circuit element voltammograms, a background subtraction method was applied to remove the circuit element component from the buffer solution, as is performed for conventional FSCV,[35] as shown in Figure 2C. As a result, the R_{ct} voltammogram showed a sharp increase at around 0.7 V. We assumed that the DA redox response would mainly appear in the R_{ct} voltammogram because R_{ct} is theoretically considered to reflect Faradic current information among the equivalent circuit components. However, the changes in the R_s and C_{dl} voltammograms induced by the injection of DA were also observed, as shown in Figure 2C. The fundamental concept of double-layer capacitance (C_{dl}) would be expected to be independent of Faradic reactions since it is assumed that the concentration of the redox species is much smaller than the concentration of the solvent molecules.[36] The change in C_{dl} from DA might be due to a pseudocapacitive change in the Faradic reaction, which was reported in a recent SCV-FTEIS study.[37] Solution resistance R_s would also be expected to have a static value during the Faradic reaction, but a voltammogram change was observed during the DA oxidation. Although R_{ct} is known as a Faradic component and is commonly measured for estimating the Faradic component in impedimetric sensors,[9] the other components, R_s and C_{dl}, also contributed to the Faradic component.[30]

Sensitivity of FTEIS−FCSWV for DA. To validate the DA detection performance of FTEIS−FCSWV, the signal-concentration linearity of FTEIS−FCSWV measurements for DA was tested using a range of physiologically relevant DA concentrations (0.5, 1.0, 1.5, and 2.0 μM). As shown in Figure 3, three circuit element voltammograms (R_{ct}, R_s, and C_{dl} voltammograms) showed significant linear peak increases proportional to the DA concentration. We also performed a limit of detection (LOD) comparison between FSCV and FTEIS−FCSWV to compare the sensitivity of the methods to DA. The experimental results showed that the LOD for FSCV was 35.8 ± 17.4 nM. For FTEIS−FCSWV circuit components, the LOD of R_{ct} was 21.6 ± 15.8 nM, the LOD of R_s was 24.2 ± 27.3 nM, and the LOD of C_{dl} was 14 ± 5 nM (n = 7 electrodes). Among the three circuit elements, C_{dl} showed the lowest sensitivity to DA. This result can be attributed to the large square wave amplitude (E_{sw} = 0.4 V), which leads to a redox chain reaction since the magnitude of E_{sw} covered the DA oxidation and reduction potentials within a single square wave pulse.[20,38,39] The coefficient of variance (the ratio of the standard deviation to the mean) was calculated from each circuit element data to examine the variation in the data (Figure S-5).

Selectivity of FTEIS−FCSWV for DA. The proposed FTEIS−FCSWV voltammograms have peaks at specific potentials. This indicates that the FTEIS−FCSWV voltammogram can be treated as conventional FSCV voltammograms and can be used to identify various neurochemicals.[40] Equivalent circuit voltammograms for DA, NE, and EP were investigated. Due to their structural similarity, the FSCV voltammogram patterns of catecholamines (DA, NE, and EP) showed almost identical redox voltammograms and, therefore, it has been challenging to differentiate these catecholamines in a mixed environment.[28,41,42] The voltammogram patterns for DA and NE using FTEIS−FCSWV were also similar, but the peak potentials were shifted because both neurotransmitters

https://doi.org/10.1021/acs.analchem.1c02308
Anal. Chem. 2021, 93, 15861−15869

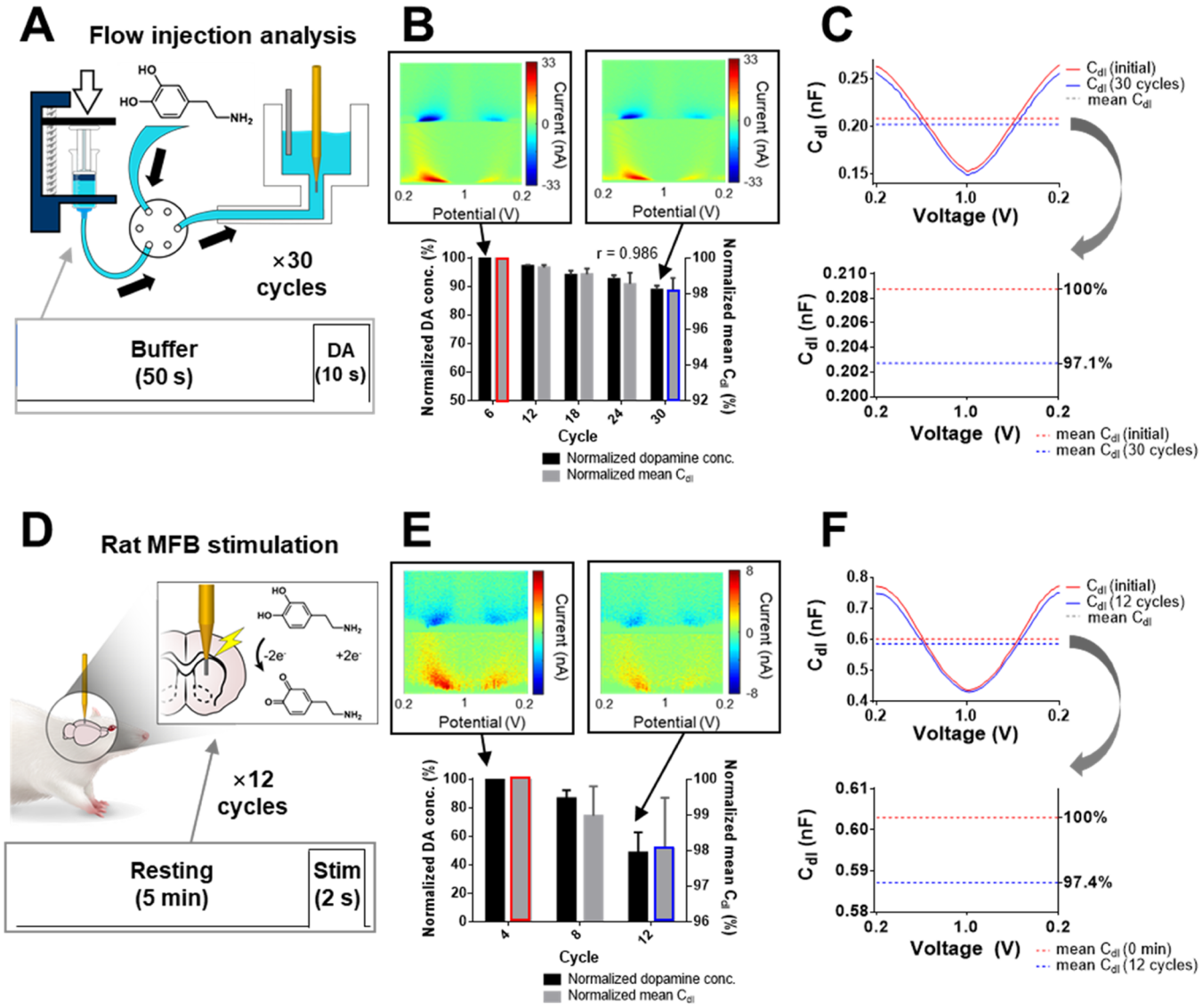

Figure 5. Relation between biofouling and double-layer capacitance(C_{dl}). (A) Repeated injection of DA based on the flow-cell experiment for inducing biofouling of the electrode. (B) Significant correlation between normalized C_{dl} and normalized dopamine response over 30 cycles (r = 0.986). FCSWV 2D voltammograms are shown. All six cycles are averaged in the graph. (C) Double-layer capacitances of first and last DA injection. Dotted lines are the averaged value of C_{dl} over all voltages. (D) *In vivo* repeated DA experiment with medial forebrain bundle stimulation. (F) Normalized C_{dl} and normalized dopamine response over 12 cycles. (F) Double-layer capacitances of first and last MFB stimulation.

have catechol structures and contain the same electrochemical functional groups (two, OH, hydroxyls and one, NH_2, amine). (Figure S-6) However, the DA oxidation peak potential was a few tens of millivolts lower than that for the NE peak potential due to the faster response for DA oxidation within the upward potential compared to the NE response, likely due to the additional hydroxyl on the β carbon of the ethylamine side chain of NE. The equivalent circuit voltammograms for EP were different from DA and NE because of the different functional groups (NCH_3, methylamine).

The FTEIS−FCSWV selectivity performance for DA was further compared with FSCV using mixtures of catecholamines by evaluating the effectiveness of additional information obtained from FTEIS−FCSWV using principal component regression (PCR). The PCR predictive performance of FTEIS−FCSWV was examined using unknown mixtures of two analytes (1 μM DA + 2 μM EP, 1 μM DA + 1 μM NE, and 1 μM NE + 2 μM EP). Among the equivalent circuit component, R_{ct} was chosen as a key parameter for the PCR analysis since R_{ct} is the equivalent circuit element correlated to the Faradic current. The root-mean-square error (RMSE) was calculated for DA, EP, and NE to evaluate the error between the estimated concentration and an actual concentration. As shown in Figure 4, the RMSE of FTEIS−FCSWV was lower than that for FSCV in the DA and EP mixture (n = 5, two-tailed t-test, $P < 0.05$) and in the NE and EP mixture ($P < 0.01$), indicating that FTEIS−FCSWV showed better selectivity compared to FSCV. Circuit element voltammograms have similar redox peak features to those for cyclic voltammetry, but the element voltammogram describes the redox reaction from a different point of view. The FTEIS in the FTEIS−FCSWV analysis describes the values for the equivalent circuit for an element, including the redox reaction and environmental change (double layer and solution resistance). This additional electrochemical information might be useful in terms of predictive performance.

https://doi.org/10.1021/acs.analchem.1c02308
Anal. Chem. 2021, 93, 15861−15869

Estimation of the Biofouling of the Electrode using Double-Layer Capacitance. Biofouling, adsorption of biomolecules and byproducts of a redox reaction, yields decreasing electrode sensitivity due to electrode surface change.[43,44] The correlation between the sensitivity decrease caused by biofouling and the C_{dl} change was investigated.[22,23]

A flow-cell injection experiment was performed for the adsorption of dopamine byproducts from oxidation, decreasing DA sensitivity. A flow injection of dopamine 1.0 μM was injected for 10 s every 1 min, a total of 30 cycles, as shown in Figure 5A. Staircase waveform parameter E_{peak} was changed to 0.6 V to induce more biofouling on the electrode.

Repeated injection of dopamine resulted in an average 14.9% decrease in the sensitivity against dopamine, while C_{dl} decreased an average of 2.5%. The Pearson correlation between sensitivity and C_{dl} was significant (r = 0.986) (Figure 5B,C). In addition, we conducted a serotonin biofouling experiment, resulting in an average 28.1% decrease in the sensitivity and an average 5.5% decrease in C_{dl} (Figure S-7). The correlation coefficient was 0.996. The results suggest that the change rate of C_{dl} can be used as an indicator for the biofouling of the electrode during the electrochemical measurement.

The *in vivo* experiment also proceeded to observe the feasibility of C_{dl} for estimating the biofouling (Figure 5D). We mimicked the flow-cell experiment with repeated DA release in the rat striatum (ML 2.0 mm, AP 1.2 mm, DV 4.5 mm) in response to brief electrical stimulation of the medial forebrain bundle containing DA axons projecting to the striatum (stimulation parameters: 350 μA, biphasic pulses, 2 ms pulse width, 60 Hz, 2 s stimulation duration). As shown in Figure 5E,F, the decreased C_{dl} was observed with the decrease in DA sensitivity as the stimulation was repeated. This could be one of the main advantages of FTEIS−FCSWV in the aspect that it could simultaneously offer a new type of neurochemical voltammogram (Figures S-8 and S-9) and the information of electrode surface like biofouling.

CONCLUSIONS

In this study, we report on the development of new types of equivalent circuit element voltammograms by applying FTEIS analysis to FCSWV, which has advantages in sensitivity and selectivity compared to FSCV. The equivalent circuit element voltammograms successfully showed that they increase linearly with the concentration of DA. This approach can be used as a new feature, similar to a conventional voltammogram from cyclic voltammetry. Finally, we demonstrated that FTEIS−FCSWV could measure the degree of biofouling on the electrode, which induces decreasing DA sensitivity. In conclusion, FTEIS−FCSWV can provide additional voltammogram features that can be useful for estimating the concentration of electroactive neurochemicals using EIS measurements with fast temporal resolution and also provide the impedance information, which can be used to evaluate the sensitivity loss caused by biofilm formation on the electrode surface.

ASSOCIATED CONTENT

Supporting Information

The Supporting Information is available free of charge at https://pubs.acs.org/doi/10.1021/acs.analchem.1c02308.

Figure S-1: Parallel computation for the faster FTEIS process; Figure S-2: Carbon-fiber microelectrode fabrication process; Figure S-3: Immittance data as impedance form and admittance form; Figure S-4: Correction process of admittance data; Figure S-5: Calibration curves of the circuit elements; Figure S-6: Equivalent circuit voltammograms of catecholamines; Figure S-7: Flow injection experiment using serotonin solution; Figure S-8: Evaluation of FTEIS−FCSWV for determining DA *in vivo*, and Figure S-9: Equivalent circuit voltammogram during the *in vivo* experiment (PDF)

AUTHOR INFORMATION

Corresponding Author

Dong Pyo Jang − *Department of Biomedical Engineering, Hanyang University, Seoul 04763, Republic of Korea;* Present Address: Fusion Tech Center 1106, Hanyang AQ6: Please confirm the postal code given to the present address for author [Dong Pyo Jang] is correct.University, 222, Wangsimni-ro, Seongdong-gu, Seoul 04763, South Korea; orcid.org/0000-0002-2832-2576; Email: dongpyojang@hanyang.ac.kr

Authors

Cheonho Park − *Department of Biomedical Engineering, Hanyang University, Seoul 04763, Republic of Korea*

Sangmun Hwang − *Department of Biomedical Engineering, Hanyang University, Seoul 04763, Republic of Korea*

Yumin Kang − *Department of Biomedical Engineering, Hanyang University, Seoul 04763, Republic of Korea;* orcid.org/0000-0002-2758-2202

Jeongeun Sim − *Department of Biomedical Engineering, Hanyang University, Seoul 04763, Republic of Korea*

Hyun U. Cho − *Department of Biomedical Engineering, Hanyang University, Seoul 04763, Republic of Korea*

Yoonbae Oh − *Department of Neurologic Surgery, Mayo Clinic, Rochester, Minnesota 55905, United States; Department of Biomedical Engineering, Mayo Clinic, Rochester, Minnesota 55905, United States;* orcid.org/0000-0003-1779-978X

Hojin Shin − *Department of Neurologic Surgery, Mayo Clinic, Rochester, Minnesota 55905, United States;* orcid.org/0000-0001-6095-5122

Do Hyoung Kim − *Nu Eyne Co., Ltd., Seoul 06604, Korea*

Charles D. Blaha − *Department of Neurologic Surgery, Mayo Clinic, Rochester, Minnesota 55905, United States*

Kevin E. Bennet − *Department of Neurologic Surgery, Mayo Clinic, Rochester, Minnesota 55905, United States; Division of Engineering, Mayo Clinic, Rochester, Minnesota 55905, United States*

Kendall H. Lee − *Department of Neurologic Surgery, Mayo Clinic, Rochester, Minnesota 55905, United States; Department of Biomedical Engineering, Mayo Clinic, Rochester, Minnesota 55905, United States*

Complete contact information is available at: https://pubs.acs.org/10.1021/acs.analchem.1c02308

Author Contributions

C.P., S.H., and Y.K. contributed equally to this work. This manuscript was written through contributions of all authors.

https://doi.org/10.1021/acs.analchem.1c02308
Anal. Chem. 2021, 93, 15861−15869

All authors have given approval to the final version of the manuscript.

Notes

The authors declare no competing financial interest.

■ ACKNOWLEDGMENTS

This work was supported by the National Research Foundation of Korea (NRF) grant (NRF-2021R1A2B5B02002437), the National Institute of Health (NIH) R01NS112176 award, Minnesota Partnership for Biotechnology and Medical Genomics Grant MNP (#19.13), and a grant from the Korean Health Technology R&D Project through the Korea Health Industry Development Institute (HI19C0753).

■ REFERENCES

(1) Macdonald, D. D. *Electrochim. Acta* **2006**, *51*, 1376−1388.
(2) Chang, B. Y.; Park, S. M. *Anal. Chem.* **2007**, *79*, 4892−4899.
(3) Macdonald, J. R.; Barsoukov, E. *Impedance Spectroscopy: Theory, Experiment, and Applications*, 2nd ed.: John Wiley & Sons, Inc.: Hoboken, NJ, 2005; Vol. *1*, p 13.
(4) Darowicki, K.; Orlikowski, J.; Arutunow, A.; Jurczak, W. *J. Electrochem. Soc.* **2007**, *154*, C74−C80.
(5) Arutunow, A.; Darowicki, K. *Electrochim. Acta* **2008**, *53*, 4387−4395.
(6) Dylla, A. G.; Lee, J. A.; Stevenson, K. J. *Langmuir* **2012**, *28*, 2897−2903.
(7) Ding, J. W.; Chen, Y.; Wang, X. W.; Qin, W. *Anal. Chem.* **2012**, *84*, 2055−2061.
(8) Smith, D. E. *Anal. Chem.* **1976**, *48*, 221A−240A.
(9) Chang, B. Y.; Park, S. M. *Annu. Rev. Anal. Chem.* **2010**, *3*, 207−229.
(10) Yoo, J. S.; Park, S. M. *Anal. Chem.* **2000**, *72*, 2035−2041.
(11) Yoo, J. S.; Song, I.; Lee, J. H.; Park, S. M. *Anal. Chem.* **2003**, *75*, 3294−3300.
(12) Garland, J. E.; Pettit, C. M.; Roy, D. *Electrochim. Acta* **2004**, *49*, 2623−2635.
(13) Arutunow, A.; Darowicki, K. *Electrochim. Acta* **2009**, *54*, 1034−1041.
(14) Chang, B. Y.; Ahn, E.; Park, S. M. *J. Phys. Chem. C* **2008**, *112*, 16902−16909.
(15) Chang, B. Y.; Lee, H. J.; Park, S. M. *Electroanalysis* **2011**, *23*, 2070−2078.
(16) Chang, B.-Y.; Park, S.-M. *J. Phys. Chem. C* **2012**, *116*, 18270−18277.
(17) Yang, Cj.; Ko, Y.; Park, S.-M. *Electrochim. Acta* **2012**, *78*, 615−622.
(18) Nam, K. M.; Shin, D. H.; Jung, N.; Joo, M. G.; Jeon, S.; Park, S. M.; Chang, B. Y. *Anal. Chem.* **2013**, *85*, 2246−2252.
(19) Michael, A. C.; Borland, L. M. *Electrochemical Methods for Neuroscience*; CRC Press, 2007.
(20) Park, C.; Oh, Y.; Shin, H.; Kim, J.; Kang, Y.; Sim, J.; Cho, H. U.; Lee, H. K.; Jung, S. J.; Blaha, C. D.; Bennet, K. E.; Heien, M. L.; Lee, K. H.; Kim, I. Y.; Jang, D. P. *Anal. Chem.* **2018**, *90*, 13348−13355.
(21) Córdoba-Torres, P.; Mesquita, T. J.; Nogueira, R. P. *J. Phys. Chem. C* **2015**, *119*, 4136−4147.
(22) Kim, T.; Kang, J.; Lee, J.-H.; Yoon, J. *Water Res.* **2011**, *45*, 4615−4622.
(23) Kim, S.; Yu, G.; Kim, T.; Shin, K.; Yoon, J. *Electrochim. Acta* **2012**, *82*, 126−131.
(24) Sekar, N.; Ramasamy, R. P. *J. Microb. Biochem. Technol.* **2013**, *6*, No. 004.
(25) Heien, M. L.; Johnson, M. A.; Wightman, R. M. *Anal. Chem.* **2004**, *76*, 5697−5704.
(26) Bennet, K. E.; Kim, I. Y.; Lee, K. H.; Jang, D. P. *Int. J. Electrochem. Sci.* **2015**, *10*, 10061−10073.
(27) Chang, S. Y.; Kim, I.; Marsh, M. P.; Jang, D. P.; Hwang, S. C.; Van Gompel, J. J.; Goerss, S. J.; Kimble, C. J.; Bennet, K. E.; Garris, P. A.; Blaha, C. D.; Lee, K. H. *Mayo Clin. Proc.* **2012**, *87*, 760−765.
(28) Kim, J.; Oh, Y.; Park, C.; Kang, Y. M.; Shin, H.; Kim, I. Y.; Jang, D. P. *Int. J. Electrochem. Sci.* **2019**, *14*, 5924−5937.
(29) Dellis, J.-L. Zfit, https://www.mathworks.com/matlabcentral/fileexchange/19460-zfit.
(30) Chang, B.-Y.; Park, S.-M. *Anal. Chem.* **2006**, *78*, 1052−1060.
(31) Orazem, M. E.; Frateur, I.; Tribollet, B.; Vivier, V.; Marcelin, S.; Pébère, N.; Bunge, A. L.; White, E. A.; Riemer, D. P.; Musiani, M. *J. Electrochem. Soc.* **2013**, *160*, C215.
(32) Schönleber, M.; Klotz, D.; Ivers-Tiffée, E. *Electrochim. Acta* **2014**, *131*, 20−27.
(33) Victoria, S. N.; Ramanathan, S. *Electrochim. Acta* **2011**, *56*, 2606−2615.
(34) Park, S.-M.; Yoo, J.-S. *Anal. Chem.* **2003**, *75*, 455A−461A.
(35) Howell, J. O.; Kuhr, W. G.; Ensman, R. E.; Wightman, R. M. *J. Electroanal. Chem. Interfacial Electrochem.* **1986**, *209*, 77−90.
(36) Aoki, K. J.; Chen, J.; Zeng, X.; Wang, Z. *RSC Adv.* **2017**, *7*, 22501−22509.
(37) Ko, Y.; Park, S.-M. *J. Phys. Chem. C* **2012**, *116*, 7260−7268.
(38) Shin, H.; Oh, Y.; Park, C.; Kang, Y.; Cho, H. U.; Blaha, C. D.; Bennet, K. E.; Heien, M. L.; Kim, I. Y.; Lee, K. H.; Jang, D. P. *Anal. Chem.* **2020**, *92*, 774−781.
(39) Oh, Y.; Heien, M. L.; Park, C.; Kang, Y. M.; Kim, J.; Boschen, S. L.; Shin, H.; Cho, H. U.; Blaha, C. D.; Bennet, K. E.; et al. *Biosens. Bioelectron.* **2018**, *121*, 174−182.
(40) Venton, B. J.; Cao, Q. *Analyst* **2020**, *145*, 1158−1168.
(41) Park, J.; Aragona, B. J.; Kile, B. M.; Carelli, R. M.; Wightman, R. M. *Neuroscience* **2010**, *169*, 132−142.
(42) Keithley, R. B.; Wightman, R. M.; Heien, M. L. *TrAC, Trends Anal. Chem.* **2009**, *28*, 1127−1136.
(43) Puthongkham, P.; Venton, B. J. *Analyst* **2020**, *145*, 1087−1102.
(44) Dunham, K. E.; Venton, B. J. *Analyst* **2020**, *145*, 7437−7446.

https://doi.org/10.1021/acs.analchem.1c02308
Anal. Chem. 2021, 93, 15861−15869